INRIA

INSTITUT NATIONAL DE RECHERCHE EN INFORMATIQUE ET EN AUTOMATIQUE

Finite element simulation of environmental flows with free boundaries

Giovanni M. CORNETTI

N° 2456
Janvier 1995

PROGRAMME 6

FINITE ELEMENT SIMULATION OF ENVIRONMENTAL FLOWS WITH FREE BOUNDARIES

Giovanni M. Cornetti

Projet Menusin, INRIA, Domaine de Voluceau - Roquencourt B.P.105, 78153 Le Chesnay France.
E-mail: cornetti@menusin.inria.fr

Abstract. The 3D Navier-Stokes equations are solved via the Characteristic-Galerkin method extended to free boundary problems. A single layer of finite elements is not sufficient to cover the 2D shallow water models. The correct behavior in the shallow water limit is obtained by two layers, where the lower one takes into account the boundary layer at the bottom wall. An application to propagating fronts generated by earthquakes on the sea bottom is proposed.

SIMULATION NUMERIQUE AVEC LA METHODE D'ELEMENTS FINIS D'ECOULEMENTS NATURELS AVEC FRONTIERE LIBRE

Résumé. Les équations de Navier-Stokes tridimensionelles sont résolues par la méthode des caractéristiques étendue aux problèmes à frontières libres. Une seule couche d'éléments finis n'est pas suffisante pour recouvrir les modèles 2D pour les eaux peu profondes. On obtient le comportement correct dans la limite des eaux peu profondes avec deux couches, la couche inférieure prenant en compte la couche limite sur le fond. Une application pour les fronts de propagation générés par des tremblements de terre sur les fonds marins est proposée.

KEY WORDS: Fluid mechanics, Environmental flows, Incompressible Navier-Stokes, Free surface flows, Finite element, Characteristic-Galerkin method, Shallow water.

Table of contents

1. Introduction

In many engineering and natural systems, one dimension of the physical space is much smaller compared to the others, thus defining a thin domain. Well known examples are shells and plates in solid mechanics or oceans and films in fluid mechanics. Moreover large deformations or moving boundaries often complicate the computations.

To solve these kind of problems, many bidimensional (2D) approximate models are proposed in the literature. They are usally derived by asymptotic expansion of the equations in the domain thickness (c.f. Ciarlet [1] or Holm and Camassa [2]). The major drawback is that the 2D model requires hypotheses on the dependency of the solution on the third coordinate which are not always satisfied (see also Babuska [3]).

In this paper a 2D model is obtained by the 3D finite element discretization in the vertical direction. The Characteristic-Galerkin method extended to free boundary problems is applied to the solution of the incompressible Navier-Stokes equations. This results in an alternative technique to the shallow water (SW) equations for environmental applications. We discuss the following points:

- extension of the Characteristic-Galerkin method to free boundary problems;
- application of the previous method with one and two layers of finite elements;
- numerical comparison with the shallow water equations.

The method of the characteristics has been succesfully applied in conjuction with the finite elements [4,5,6] or the spectral elements technique [7]. The basic idea is to perform convection trasporting the velocity value back in time along the trajectory. It can be also interpreted as a splitting method, one step of transport plus one step of diffusion, because it looks as if first the velocity is convected and then diffused. One of the major advantage of the method is its great stability. This results in considerable time saving when the phenomena are mainly convective, as in free surface wave propagation.

In free boundary problems, the convection cannot be carried out in an explicit fashon along trajectories, which may exit the computational domain. The standard Characteric-Galerkin discretization has to be adapted using an arbitrary Lagrangian Eulerian (ALE) formulation, where physical variables are convected by vector fields tangential to the free surface. The price one pays is that an additional source term appears, that depends on the divergence of the new field.

When the domain is thin in one Cartesian direction, e.g. the vertical, it is straightforward to move the mesh points in that direction. For this case a detailed temporal discretization scheme is proposed and consistency errors analysed.

The last part of the paper is dedicated to numerical examples. For a solitary wave propagating along a constant depth channel, the computed solution is in a good agreement with the one-dimentional Korteg de Vries (KdV) equations, when

two layers of finite elements are used. The problem of the validity of the model (see Holm and Camassa [2]) is changed to a numerical approximation problem, but these are well understood. Furthermore the numerical discretization scheme presented is more widerly applicable then the SW equations used in practical computation[8,9]. For instance, it can be employed to track a propagating front generated by earthquake on the sea bottom. The method seems to be competitive with actual codes based on the 2D model approximation. In addition, the mesh can be refined locally in depth, thereby enhancing the solution accuracy when needed.

2. Problem's definition

In the incompressible Navier-Stokes equations with free boundary, the computational domain $\Omega(t) \subset I\!R^3, t \in]0,T[$ is unknown. An additional condition for the free surface $\Gamma_f(t)$ states that $\Gamma_f(t)$ is a material surface. Let ω be an open subset of $I\!R^2$ and, for $t \in]0,T[$, consider

$$\Omega(t) = \{x = (y,z) : y \in \omega, \eta > z > -H\},$$

where $z = -H(y)$ is the equation of the bottom and $z = \eta(y,t)$ the equation of the free-surface $\Gamma_f(t)$, so that $h = \eta + H$ is the total depth. The free boundary condition may be written as

$$D_t\eta = \partial_t\eta + u_{12} \cdot \nabla\eta = u_3 \quad \text{on } \Gamma_f(t), \tag{2.1}$$

with u_{12} the horizontal and u_3 the vertical velocity components. Equation (2.1) does not allow wave breaking phenomena, because η is a single-valued function. Hereafter D_t,∂_t denote the total and the partial time derivative.

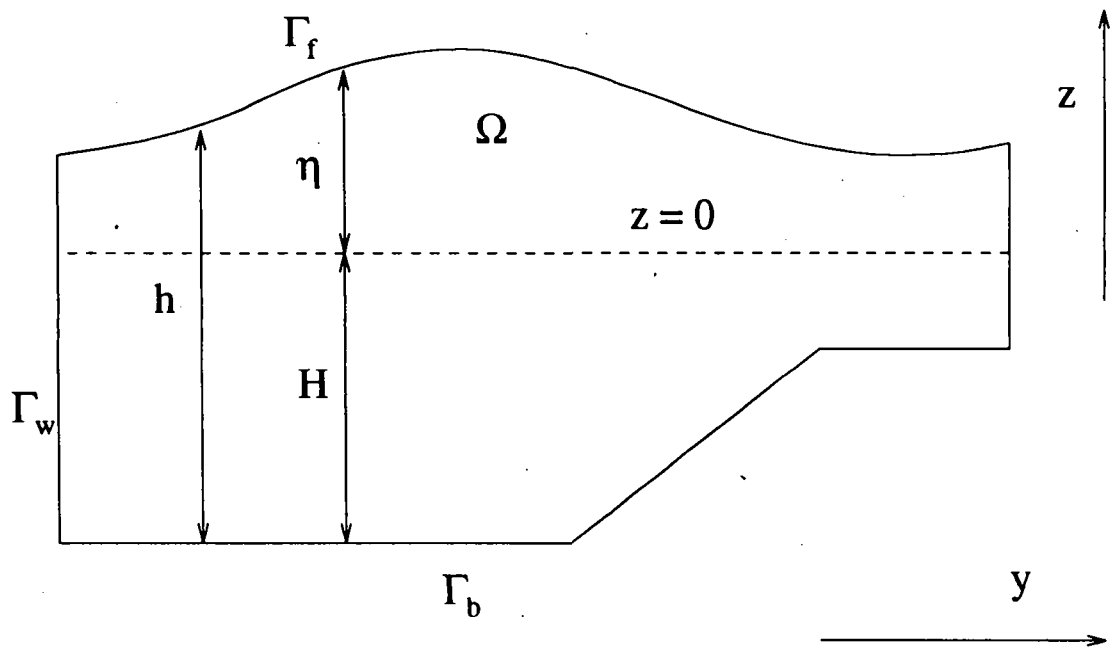

Fig.1. *The geometry of the fluid layer.*

The boundary of the domain is decomposed as follows:

$$\partial\Omega(t) = \Gamma_w(t) \cup \Gamma_b \cup \Gamma_f(t)$$

$$\begin{aligned} \text{side wall} \quad & \Gamma_w(t) = \{x = (y,z) : y \in \partial\omega, \eta > z > -H\}, \\ \text{bottom} \quad & \Gamma_b = \{x = (y,z) : y \in \omega, z = -H\}, \\ \text{free surface} \quad & \Gamma_f(t) = \{x = (y,z) : y \in \omega, z = \eta\}. \end{aligned}$$

Moreover it is useful to define the space-time domain

$$\mathcal{D} = \{x, t : x \in \Omega(t), t \in]0, T[\}.$$

For a viscous incompressible Newtonian fluid under the influence of gravity, the mass and momentum equations in a time dependent domain $\Omega(t)$ are:

$$\begin{aligned} \partial_t u + u \cdot \nabla u + \nabla(p + gz) - \nu\Delta u = 0 \quad & \text{in } \mathcal{D}, \\ \nabla \cdot u = 0 \quad & \text{in } \mathcal{D}. \end{aligned} \tag{2.2a}$$

In practical computations, the following boundary conditions will be useful:

$$\begin{aligned} \text{inflow,outflow} \quad & (u_1, u_2) = (u_{\Gamma 1}, u_{\Gamma 2}), -\nu\frac{\partial u_3}{\partial n} = 0 \quad \text{on } \Gamma_u(t), \\ \text{radiating} \quad & -\nu\frac{\partial u}{\partial n} + (p + gz)n = g\eta n \quad \text{on } \Gamma_p(t), \\ \text{bottom} \quad & u = 0 \quad \text{on } \Gamma_b, \\ \text{free surface} \quad & -\nu\frac{\partial u}{\partial n} + (p + gz)n = g\eta n \quad \text{on } \Gamma_f(t), \end{aligned} \tag{2.2b}$$

with $\Gamma_w(t) = \Gamma_u(t) \cup \Gamma_p(t)$. The initial condition is

$$u = 0 \quad \text{in } \Omega(0). \tag{2.2c}$$

Here $u = (u_1, u_2, u_3)$ is again the velocity, g the acceleration of gravity, p the pressure and $(u_{\Gamma 1}, u_{\Gamma 2})$ are the prescribed horizontal components of the velocity on the side wall $\Gamma_u(t)$. Furthermore, ν is the kinematic viscosity and n the outward pointing normal to $\partial\Omega(t)$. The flow is able to slip along the side wall in the vertical direction, and, on $\Gamma_f(t)$ and Γ_p, the surface tension and the tangential stresses are neglected.

In environmental flows Γ_u represents the inflow and outflow boundaries, or for $u_{\Gamma 1} = u_{\Gamma 2} = 0$ the shoreline, and Γ_p the open sea, where no stress is prescribed on the border. The last condition allows surface waves to radiate out of the domain without being reflected.

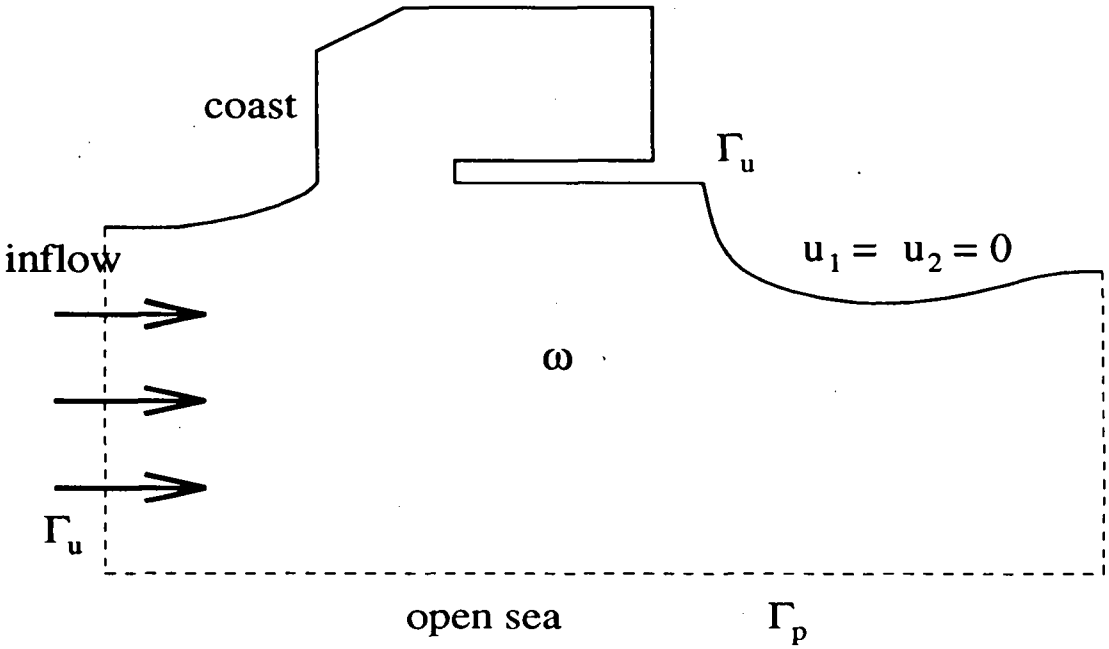

Fig.2. *Typical boundary conditions for flow field computation near the coast (2D view from above).*

3. Temporal discretization

A suitable discretization of the time parameter along streamlines is based on the method of characteristics. This is a splitting technique that decouples the convection part and the viscous part. In the case of a free surface problem and time dependent domain, at each time step δt, the new mesh points, velocity and

pressure are updated first by solving two convection equations

$$\partial_t \eta + u_{12} \cdot \nabla \eta = u_3,$$
$$\partial_t u + u \cdot \nabla u = 0,$$

and then a Stokes type problem

$$\frac{1}{\delta t} u + \nabla p - \nu \Delta u = f,$$
$$\nabla \cdot u = 0,$$

taking for initial value the result of the convection step.

The computational scheme used to solve the time dependent free boundary problem in thin domain is presented. It can be summarized as follows:

step 1) approximation of the total derivative;
step 2) update of the computational domain;
step 3) solution of an implicit Stokes problem.

The procedure is iterated in time.

- *Preliminaries*

Denoting $k = \delta t > 0$ the time step and the discrete time,

$$t^m = mk, \quad 0 \leq m \leq M = \frac{T}{\delta t},$$

we define Ω^m, Γ_f^m and $u^m(x)$ the approximations of $\Omega(t^m)$,$\Gamma_f(t^m)$ and $u(x,t^m)$ respectively, such that

$$\Omega^m = \{x = (y,z) : y \in \omega; \eta^m > z > -H\}.$$

Furthermore, assuming $n_3 \neq 0$ on Γ_f^m, we introduce a velocity v^m defined by:

$$v^m = u^m - \begin{pmatrix} 0 \\ 0 \\ (z+H)\beta^m \end{pmatrix} \quad \text{in } \Omega^m, \tag{3.1}$$

where

$$\beta^m = \frac{u^m \cdot n}{h^m \, n_3}, \; h^m = \eta^m + H \quad \text{on } \Gamma_f^m.$$

- *The convection step*

Compute

$$Y^m(x) = x - v^m(x)\,k \tag{3.2}$$

then, having defined $a \circ b(x)$ as $a(b(x))$, compute

$$\eta^{m+1} = \eta^m + kh^m\beta^m \circ Y^m \quad \text{on } \Gamma_f^m \tag{3.3}$$

$$\tilde{u}^m = (u^m + ku^m\beta^m) \circ Y^m \quad \text{in } \Omega^m. \tag{3.4}$$

At each time step the new domain Ω^{m+1} is set

$$\Omega^{m+1} = \{x = (y,z) : y \in \omega; \eta^{m+1} > z > -H\}.$$

- *The diffusion step*

Solve on Ω^{m+1}:

$$\begin{cases} \dfrac{1}{k}u^{m+1} - \nu\Delta u^{m+1} + \nabla(p+gz)^{m+1} = \dfrac{1}{k}\tilde{u}^m \circ Z^m \dfrac{h^m}{h^{m+1}}, \\ \nabla \cdot u^{m+1} = 0. \end{cases} \tag{3.5}$$

where $h^{m+1} = \eta^{m+1} + H$ and $Z^m : \Omega^{m+1} \to \Omega^m$ is defined at $x = (y,z)$ by

$$Z^m(x) = x + \begin{pmatrix} 0 \\ 0 \\ (z+H)\dfrac{h^m - h^{m+1}}{h^{m+1}} \end{pmatrix}.$$

It will be shown that the scheme (3.1)-(3.5) provides an $O(k^2)$ approximation of Ω^{m+1} and an $O(k)$ approximation of u^{m+1},p^{m+1} of the solution Ω,u,p, where p is defined up to a constant. The scheme is well-defined because (3.5) has a unique solution.

REMARK 3.1. The point $Y^m(x)$ is a first order approximation of the characteristic curve related to the vector field v^m. In practice, more accurate approximations need to be used, see Pironneau [7] for detail.

REMARK 3.2. By definition (3.1), v^m is tangential to the free boundary Γ_f^m. For $z + H = h^m$ we have:

$$v^m \cdot n = u^m \cdot n - \begin{pmatrix} 0 \\ 0 \\ \dfrac{u^m \cdot n}{n_3} \end{pmatrix} \cdot n = 0;$$

see figure 3. Formula (3.2) gives $Y^m(\Omega^m) = \Omega^m + 0(k^2)$.

REMARK 3.3. The computational scheme (3.1)-(3.5) may be interpreted as an ALE formulation of the Characteristic-Galerkin method with a Lagrangian configuration moving at velocity v^m. Using (3.1), it yields $u^m = v^m + w^m$ with

$$w^m = \begin{pmatrix} 0 \\ 0 \\ (z+H)\beta^m \end{pmatrix}.$$

The only constraint for consistency is that v^m has to be tangential to Γ_f^m, namely u and w have the same normal component:

$$u^m \cdot n = w^m \cdot n \quad \text{on } \Gamma_f^m.$$

The scalar β^m has been chosen accordingly.

The direction of w^m could be imposed arbitrarily; in the scheme the vector field w^m has no horizontal component and is linear in depth: w^m is zero at the bottom. Notice also that the term β^m corresponds to the divergence of the vector field w^m, $\beta^m = \nabla \cdot w^m$.

REMARK 3.4. The point $Z(x)$ correspond to the position of x at time t^m before the vertical convection induced by the time variation of depth. In (3.4) β^m is added as a source term along the Y characteristic line, in order to take into account the changes of volume associated to the convection of the free surface.

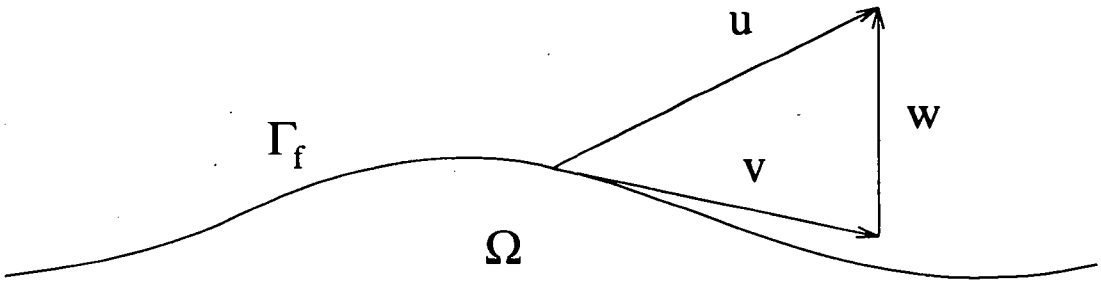

Fig. 3. *The ALE formulation: the velocity field v is tangential to the free boundary Γ_f.*

4. Consistency properties

In the space-time slab

$$\mathcal{D}^m = \{(x,t) \in \mathcal{D}, t \in [t^n, t^{n+1}[\subset [0,T[\}$$

the characteristic line X is introduced:

$$\frac{\partial X}{\partial t}(x,t) = u(X,t), \quad X(x,t^{m+1}) = x. \tag{4.1}$$

Let the mappings Z and Y be: $Z : \Omega(t^{m+1}) \to \Omega(t^m)$

$$Z(x) = x + \begin{pmatrix} 0 \\ 0 \\ (z+H)\dfrac{h(y,t^m) - h(y,t^{m+1})}{h(y,t^{m+1})} \end{pmatrix}$$

with $x = (y,z)$, and $Y : \Omega(t^m) \to \Omega(t^m)$

$$Y(x) = X(Z^{-1}(x), t^m).$$

The consistency error for the free boundary e_η^{m+1} is obtained as the rest of expression (3.3) when the exact solution replaces the discrete one. Therefore for $y \in \omega$ we have

$$e_\eta^{m+1}(y) = \frac{\eta(y,t^{m+1}) - \eta(y,t^m)}{k} - h(y,t^m)\beta(Y(y,\eta(y,t^m)),t^m), \tag{4.2}$$

where for $x = (y,z) \in \Omega(t)$

$$\beta(y,t) = \frac{u(y,\eta(y,t),t)\cdot n}{h(y,t^m)\, n_3}.$$

The continuous characteristic line Y cannot be defined directly from the velocity v, but the Z mapping from $\Omega(t^{m+1})$ to $\Omega(t^m)$ has to be used.

PROPERTY 4.1. *For smooth data* $e_\eta^{m+1} = O(k)$.

PROOF. The normal unit vector n to the free boundary is expressed by

$$n = \left(\frac{-\nabla\eta}{(\nabla\eta)^2+1}, \frac{1}{(\nabla\eta)^2+1}\right).$$

Thus, the free boundary condition (2.1) is equivalent to

$$\partial_t\eta = -u_{1,2}\cdot\nabla\eta + u_3 = \frac{u\cdot n}{n_3} = \beta h.$$

Therefore from (3.1)-(3.2) it yields:

$$h(y,t^m)\beta(Y(y,\eta(y,t^m)),t^m) = h(y,t^m)\beta(y,t^m) + O(k) = \\ = \partial_t\eta(y,t^m) + O(k)$$

and, substituting in (4.2), property 4.1 is proved.

■

The consistency error for the velocity e_u^{m+1} could be defined on the new domain Ω^{m+1}, neglecting a part of order $O(k^2)$ near the boundary:

(4.3)

$$e_u^{m+1}(x) = \frac{1}{k}\left[u(x,t^{m+1}) - \tilde{u}(Z(x))\frac{h(y,t^m)}{h(y,t^{m+1})}\right] + [\nabla(p+gz) - \nu\Delta u + f](x,t^{m+1}),$$

where for $x \in \Omega(t^m)$

$$\tilde{u}(x) = [u + ku\beta](Y(x),t^m).$$

PROPERTY 4.2. *For smooth data* $e_u^{m+1} = O(k)$.

PROOF. Using the Navier-Stokes equations (2.2), formula (4.3) is rewritten as

$$(4.4)\quad e_u^{m+1}(x) = \frac{1}{k}\left[u(x,t^{m+1}) - \tilde{u}(Z(x))\frac{h(y,t^m)}{h(y,t^{m+1})}\right] - [\partial_t u + u\cdot\nabla u](x,t^{m+1}).$$

Since, by definition $Y(x) = X(Z^{-1}(x),t^m)$,

$$\tilde{u}(Z(x)) = [u + ku\beta](X(x,t^m),t^m) = u(X(x,t^m),t^m) + k[u\beta](x,t^m) + O(k^2),$$

and, using

$$\frac{h(y,t^m)}{h(y,t^{m+1})} = 1 - k\beta(x,t^m) + O(k^2),$$

it yields

$$\tilde{u}(Z(x))\frac{h(y,t^m)}{h(y,t^{m+1})} = u(X(x,t^m),t^m) + k[u\beta](x,t^m) - k[u\beta](x,t^m) + O(k^2) = \\ = u(X(x,t^m),t^m) + O(k^2).$$

The last equality may be replaced in (4.4). As

$$[\partial_t u + u\cdot\nabla u](x,t^{m+1}) = \frac{\partial u(X(x,t),t)}{\partial t}\Big|_{t=t^{m+1}} = \\ = \frac{u(x,t^{m+1}) - u(X(x,t^m),t^m)}{k} + O(k),$$

the result is obtained.

■

5. Spatial discretization

The INRIA code NSp1b3 (see [10]) has been modified to incorporate moving meshes. The weak formulation of the Stokes problem (2.16) is approximated using tetrahedral elements. Let $\mathcal{T}_h^m$ a triangulation on Ω_h^m, the following finite dimension spaces are defined for velocity and pressure respectively:

$$V_h^m = \{\psi_h^m \in C^0(\Omega_h^m)^3 : \forall T \in \mathcal{T}_h, \psi_h^m|_T \in P_1 \oplus P_{4,0}(T)\},$$

$$Q_h^m = \{\phi_h^m \in C^0(\Omega_h^m) : \forall T \in \mathcal{T}_h, \phi_h^m|_T \in P_1\}.$$

The space V_h^m is enriched by fourth order polynomials with zero trace on the element border $P_{4,0}(T)$ (bubble), in order to satisfy the Babuska-Brezzi condition in the Stokes problem.

The resulting formulation of the discrete problem is then :
given Ω_h^{m+1} and $\tilde{u}_h^{m+1}$, find u_h^{m+1} and p_h^{m+1} such that for all $\psi_h^{m+1} \in V_h^{m+1}$, $\phi_h^{m+1} \in Q_h^{m+1}$:

$$(5.1)\quad \begin{cases} \dfrac{1}{k}\displaystyle\int_{\Omega_h^{m+1}} u_h^{m+1}\psi_h^{m+1} + \nu \int_{\Omega_h^{m+1}} \nabla u_h^{m+1}\nabla\psi_h^{m+1} + \\ -\displaystyle\int_{\Omega_h^{m+1}} {p_h'}^{m+1}\nabla\cdot\psi_h^{m+1} = \int_{(\Gamma_f\cup\Gamma_p)_h^{m+1}} g\eta_h^{m+1} n\ \psi_h^{m+1} + \frac{1}{k}\int_{\Omega_h^m} \tilde{u}_h^m\psi_h^m, \\ \\ \displaystyle\int_{\Omega_h^{m+1}} \nabla\cdot u_h^{m+1}\phi_h^{m+1} = 0. \end{cases}$$

where $p' = p + gz$ is the corrected pressure. The test function $\psi_h^m \in V_h^m$ is defined on the old domain, in particular

$$\psi_h^{m+1} = \psi_h^m \circ Z^m.$$

The characteristic curves Y_h^m are obtained updating the convective velocity v_h^m and the divergence term β_h^m each time the curve enters a new element. For instance, $k_i < k$ being the time for a particle to traverse the element T_i, we have

$$Y_h^m(x) = x - \sum_{i=1}^{N} k_i v_h^m|_{T_i}(x)$$

with $\sum_{i=1}^N k_i = k$. To track the free surface in time only the characteristic lines related to nodal points are used. The integral in the RHS of (5.1) is computed with a primal Gauss formula with fiften integration points ξ_i per element:

$$I^m = \int_{\Omega_h^m} \tilde{u}_h^m\psi_h^m \approx \sum w_j \tilde{u}_h^m(\xi_j)\psi_h^m(\xi_j)$$

See Zienkewicz [11] and Pironneau, Tezduyar [4] for details. To solve the linear system associated to the discrete problem (5.1) a Uzawa conjugate gradient iterative technique is employed.

-The algorithm

At each time step the following procedure is iterated recursively:

1. compute the divergence term β_h^m;
2. convect the quantities η_h^{m+1} and $\tilde{u}_h^m$, using the velocity v_h^m and adding β_h^m as a source term along the piecewise affine characteristic lines (see (2.4));
3. compute the integral I^m;
4. move mesh points according to step 2;
5. solve the Stokes problem on the new domain, using the result of step 3.

Only mesh points on the free surface are moved.

6. Solitary wave test problem

For inviscid flows, the free surface dynamics may be described by the Korteg de Vries (KdV) equation in the limit of long wave and small amplitude perturbation:

$$\mu = kH >> 1, \quad \epsilon = \frac{\eta}{H} << 1$$

where $k = 2\pi/\lambda$ is the wave number and λ the wavelength. This equation has an analytical solution, called soliton as it is represented by a single peak propagating in time. For an overwiew on the KdV and others SW equations see [12]. The surface elevation is given by

$$\eta = A\, sech \frac{x - ct}{\lambda}$$

with

$$c = \sqrt{gH(1+\epsilon)}$$

the wave propagation velocity, A a constant, and *sech* the hyperbolic secant function.

Using the previous algorithm, the propagation of a solitary wave in a constant depth channel is computed. As initial condition velocity is set to zero and the free boundary profile is given. On the side wall a slip condition is imposed in the vertical direction, while no slip condition is assumed for the bottom.

Numerical data are listed below:

Horizontal domain	$\omega =]0, 100[\times] - 5, 5[$
Initial velocity	$u = 0$
Acceleration of gravity	$g = 1$
Initial free boundary profile	$\eta(y_1, y_2) = 0.01 sech \frac{y_1}{8}$
Water depth	$H = 1$
Time step	$k = 2$

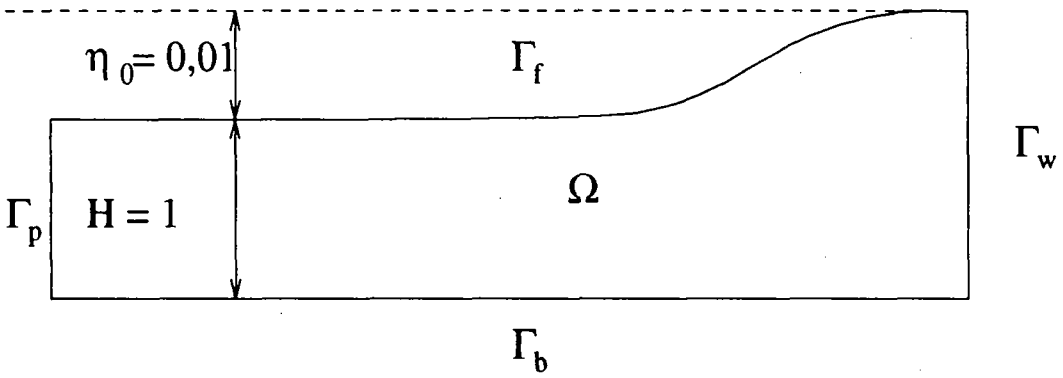

Fig. 4. *The computational domain.*

The expected wave propagation speed is

$$c = \sqrt{gH(1+\epsilon)} = 1$$

Picture 5 shows the behavior of the solitary wave in time. Only a single layer of finite elements is used, and a linear velocity profile is recovered in the vertical direction. The wave top conserves one half of the intial elevation, so that part of the potential energy is tranformed into the kinetic energy. Due to the high Reynolds number, $Re = 1000$, the wave is moving without being flattened by viscosity. The wave speed for the computed solution is

$$c = 0.89$$

which gives a relative error $e_r = 11\%$. This error is reduced to an acceptable value by the two layer discretization proposed in figure 6. In this case the wave speed rises to

$$c = 0.96$$

with a relative error $e_r = 4\%$. The horizontal velocity grows rapidly near the bottom, while the profile remains constant in the rest of the domain. The wave speed is improved, since the finer discretization captures the boundary layer on the bottom.

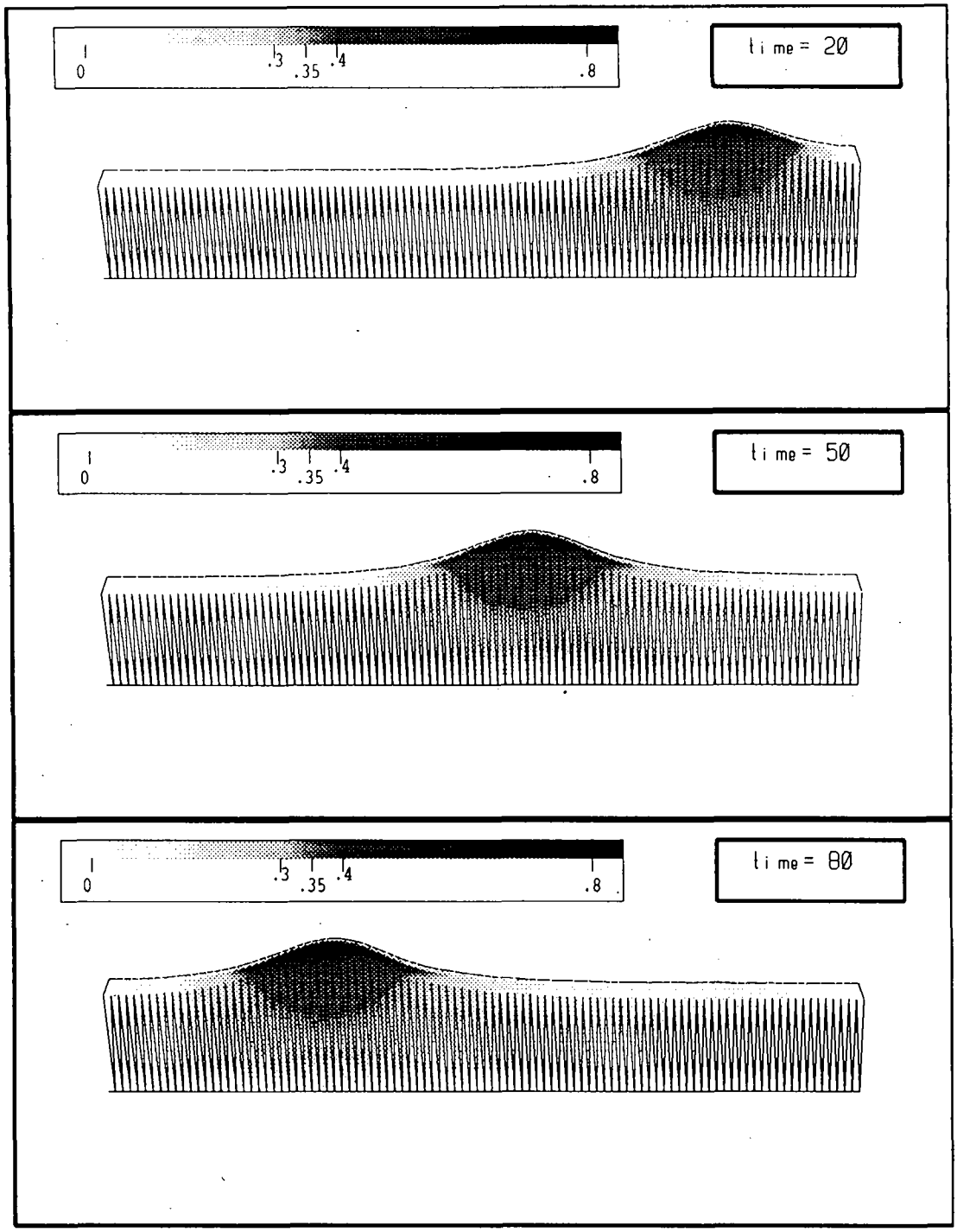

Fig. 5. *Test problem: cut view of the solution with a single layer of tetrahedral elements at three different times. The surface displacement η is magnified by a factor of 1000, and the layer thickness H by a factor of 10. The horizontal velocity scale is shown (top left).*

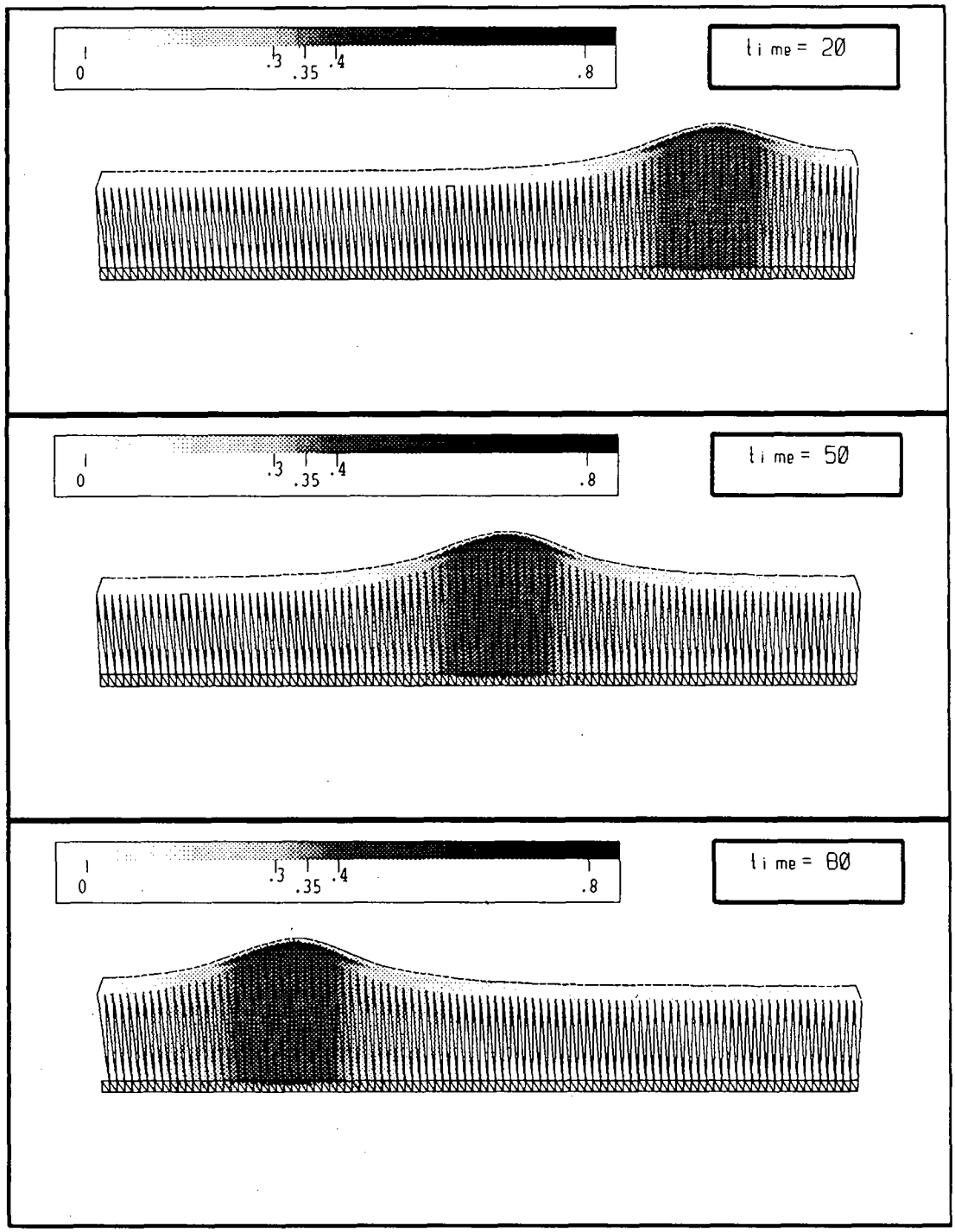

Fig. 6. *Cut view of the solution with a two layers discretization. The vertical size of the lower layer is 0.125, the total depth* $H = 1$. *A boundary layer appears on the bottom wall.*

7. Prediction of a Tsunami wave

An earthquake on the sea floor determines an instantaneous motion of the water surface. Despite its usually low amplitude (1 meter) in the deep ocean or sea, the propagating front can reach large amplitude near the coast as a consequence of refraction and local topography.

The Algeciras bay in the Mediterranean sea is used as the place for the simulation of one of these events. The computational domain, including both the bay and the epicenter, has a characteristic length of about 30 kilometers and the water surface is increased by by about 2 meters as initial condition at the epicenter.

The two layers mesh used for the finite elements discretization is given in figure 8. The lower layer is only 10 meters high, and therefore is not visible in the picture.

The magnitude of the time step is limited by a CFL condition associated to the wave propagation speed. The minimum horizontal element size $h_T = 500m$ and the maximum depth $H_{max} = 500m$ give a bound on the time step:

$$k < \frac{h_T}{\sqrt{gH_{max}}} \approx 7s.$$

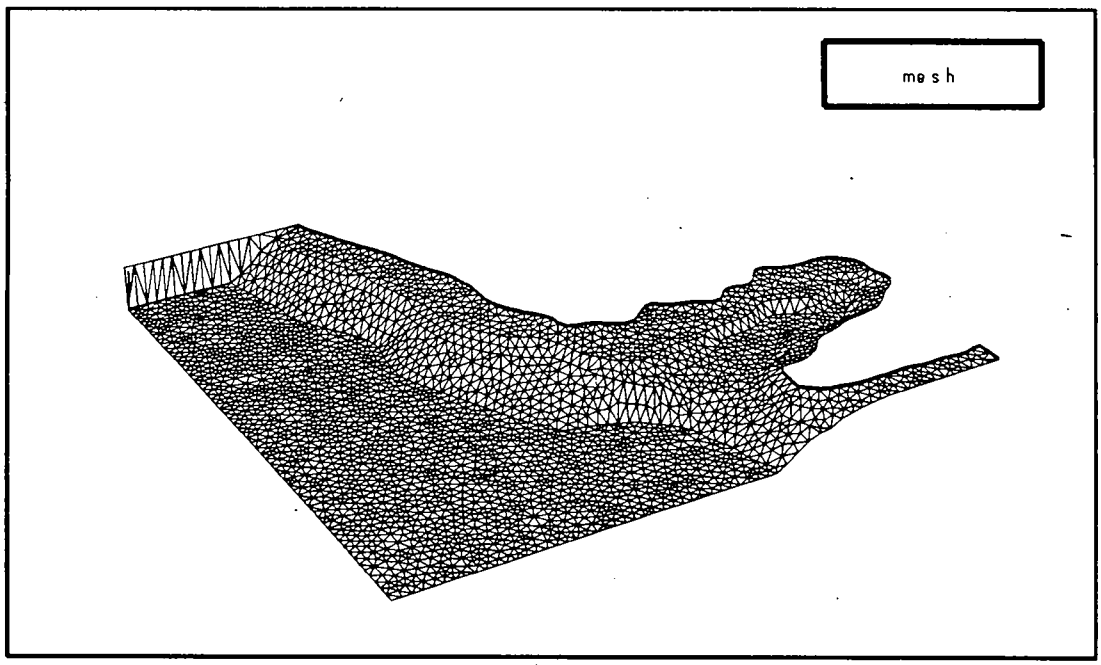

Fig. 8. *Mesh of the bottom of the computational domain. The depth is magnified by a factor of 5. Tetrahedral elements are placed in two layers; the lower layer is only 10 meters high, which is small since the maximum total depth of the domain is 500 meters.*

General data for the numerical simulation are:

Initial velocity	$u_i = 0$
Acceleration of gravity	$g = 9.8m/s$
Initial water surface elevation	$\eta_0 = 2m$
Radius of initial water surface perturbation	$r_0 = 3km$
Maximum water depth	$H_{max} = 500m$
Number of mesh points	2822×3
Time step	$k = 6s$

Figures 9 to 11 show the computed results. Grey tones illustrate surface elevation. The epicenter is located at about $12km$ from the coast in a region of $500m$ deep water. The open sea is simulated using the radiating boundary condition and on the shoreline the horizontal velocity is set to zero.

The propagating front is reflected by a sudden change in the bottom profile near the coast, see fig.10 and compare to fig.8. Therefore the maximum surface elevation on the shore is detected close to the two sides of the bay entrance, as shown in figure 10-11.

8. Conclusions

The object of the present work was to develop an efficient method for computing incompressible flow problem in a thin domain with a free boundary, without introducing a 2D asympytotic model approximation. This requires the solution of the full 3D Navier-Stokes equations plus an extra equation for the moving boundary. A good method to solve this class of problems is the Characteristic-Galerkin, extended to time dependent domains via the ALE formulation.

Two layers of finite elements have to be used to correctly simulate the boundary layer at the bottom. Then the computed solution is consistent with the SW models obtained by an asymptotic expansion in the domain thickness and valid for the long wave regime. This seems to be a very interesting result, in particular because the relationship between the FEM and asymptotic expansions is not yet theoretically proven.

Futhermore the method can be succesfully applied to the prediction of wave front generated by earthquakes on the sea floor. In particular any kind of bottom topography can be employed, since at least a single layer of three dimensional elements is used.

Acknowledgements. The author is very grateful to Professor Pironneau for the supervision of the entire work. The author wishes also to thank *Instituto Español de Oceanografía (Centro Fuengirola)* for providing me general data on the sea bottom topography near Algeciras.

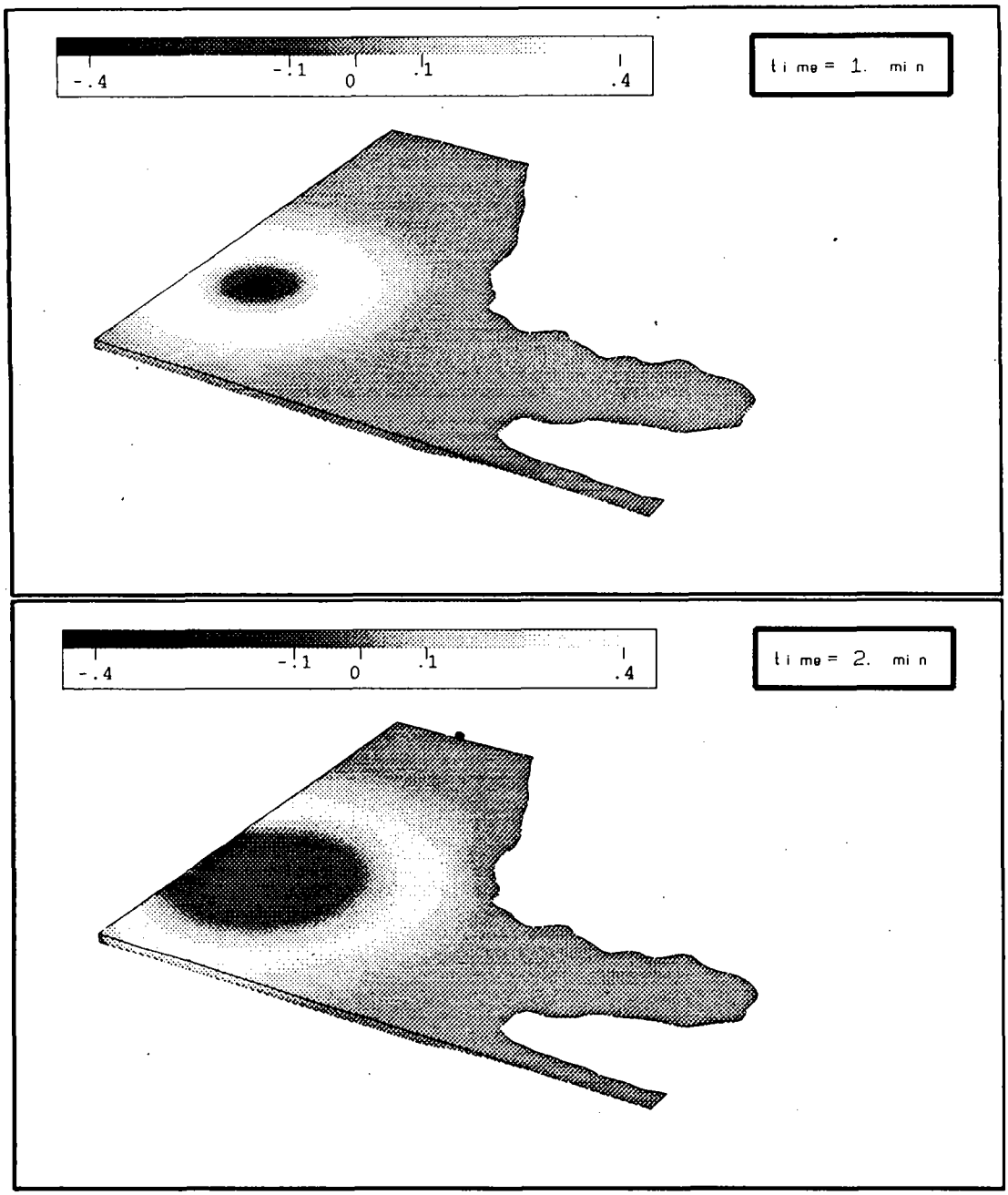

Fig. 9. *Perspective view of the solution for the Tsunami problem. As initial condition the water level is increased by 2 meters at the epicenter, located 10 kilometers off the coast. The surface elevation scale in meters (top left) and the time (top right) are shown.*

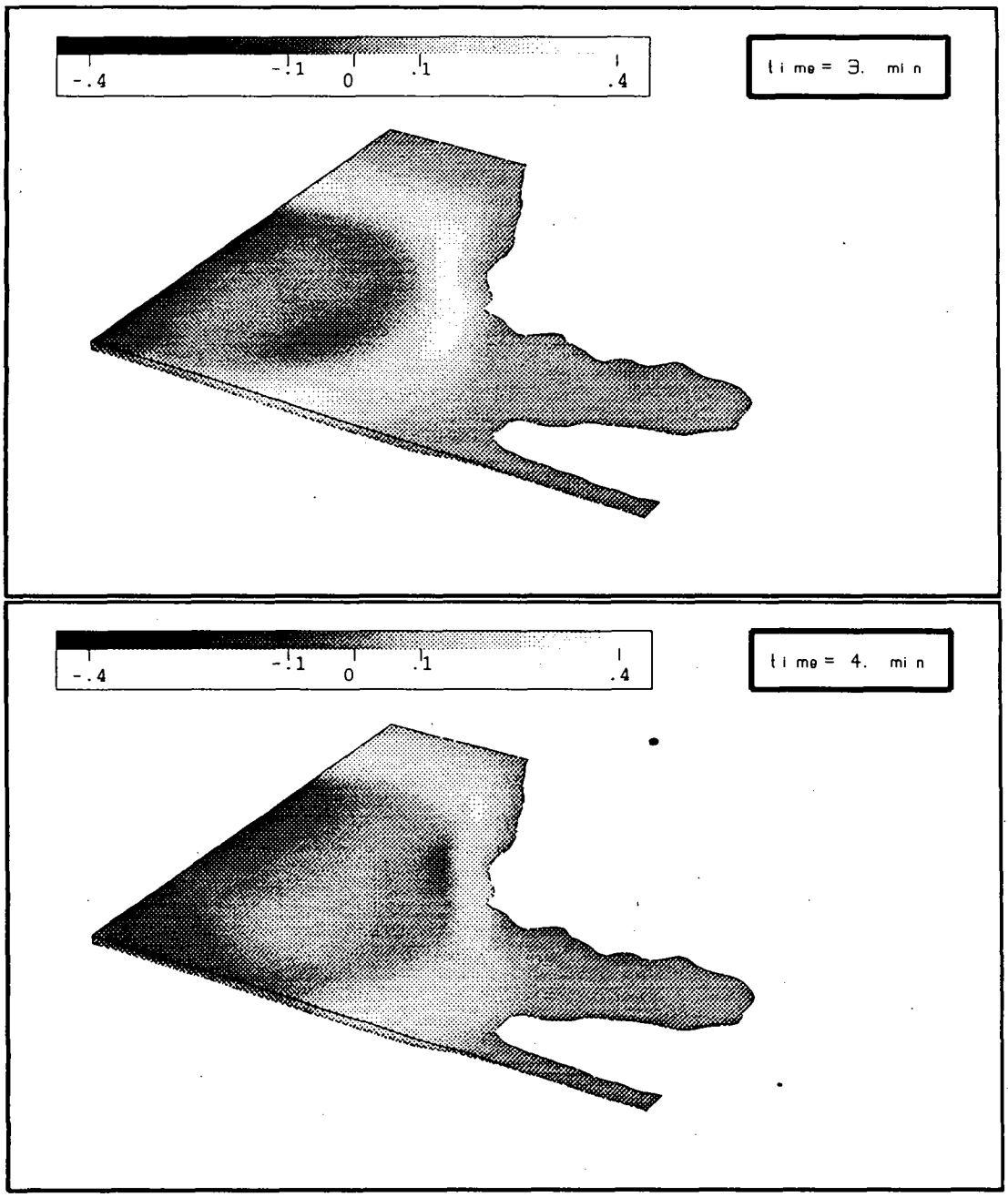

Fig. 10. *Perspective view of the solution for the Tsunami problem. Before reaching the coast, the wave front is partially reflected by the sudden change of the bottom topography.*

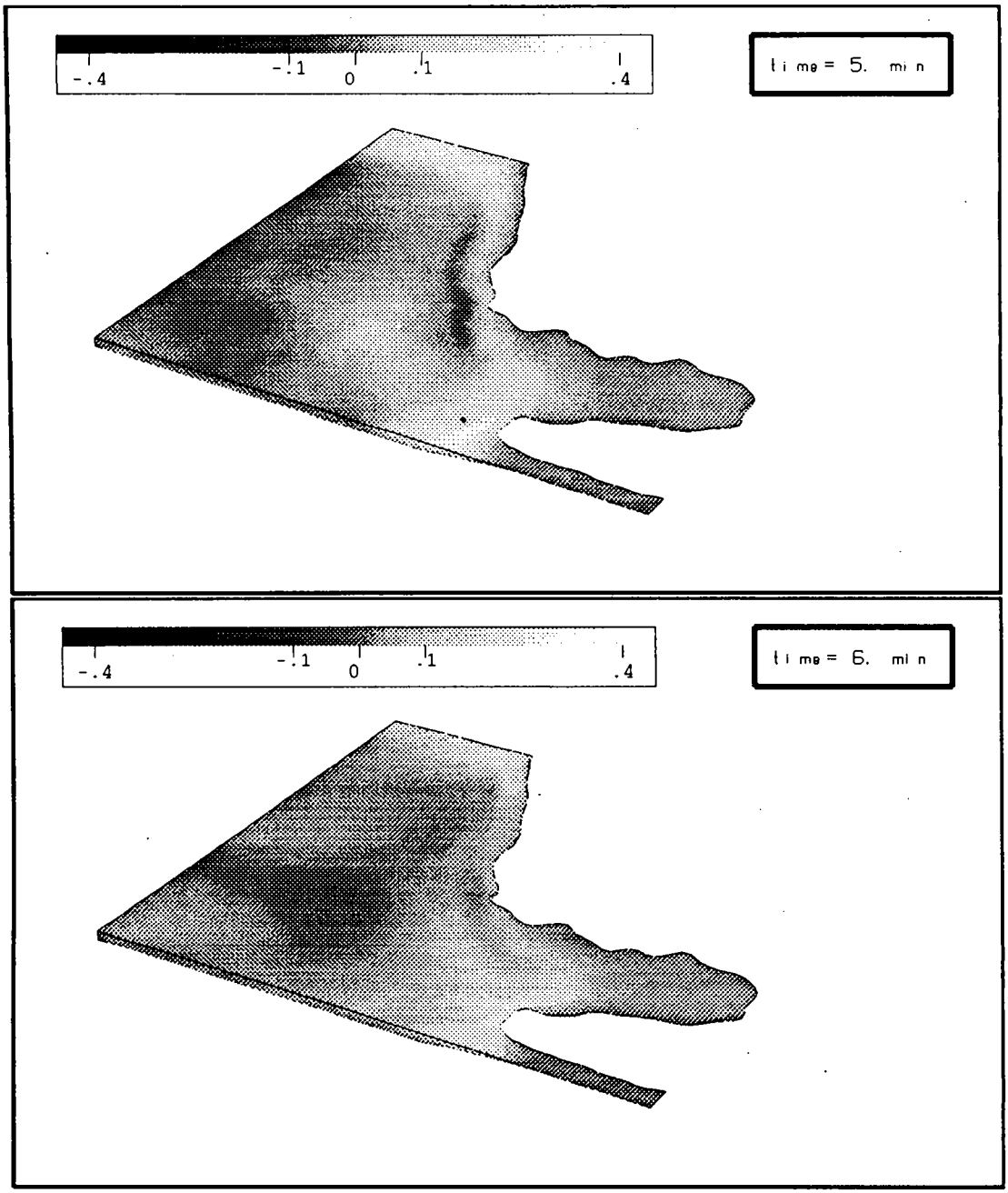

Fig. 11. *Perspective view of the solution for the Tsunami problem. The maximum surface elevation on the shore is found on each sides of the bay entrance.*

References

[1] P.G.Ciarlet, *Plates and junction in elastic multistructures: an asymptotic analysis* (Masson,Paris,1990).

[2] R.Camassa,D.D.Holm, *Dispersive barotropic equations for stratified mesoscale ocean dynamics,* Physica D 60 (1992), 1-15.

[3] I.Babuska,I.Lee,C.Schwab, *On the a posteriori estimation of the modelling error for heat conduction in a plate and its use for adaptive hierarchic modelling,* Institute for physical science and technology, University of Maryland, Technical Note BN-1145 (1993).

[4] O.Pironneau,J.Liou,T.Tezduyar, *Characteristic Galerkin and Galerkin least squares space time formulations for the advection diffusion equation with time dependent domains,* Compt. Methods Appl. Mech. Engrg. 100 (1992), 117-141.

[5] O.Pironneau, *The finite element method in fluids* (Masson, Paris, 1989).

[6] K.Boukir,Y.Maday,B.Metivet, *A high order characteristic finite element method for the incompressible Navier Stokes equations,* Int. J. Num. Meth. Fluids (to appear).

[7] L.Ho,Y.Maday,A.Patera,E.Ronquist, *An operator integration splitting method for time dependent problems. Application to incompressible fluid flows.* Jr. Sc. Comp. 5 (1990), no.4, 263-294.

[8] V.Agoshkov,E.Ovtchinnikov,V.Pennati,D.Ambrosi,F.Saleri, *Finite element, finite volume and finite differences approximation to shallow water equations,* Finite elements in fluids CIMNE Barcelona, Pineridge Press (1993), 1001-1009.

[9] M.J.Castro,C.Pares,J.Macias, *Numerical modelling of the Alboran sea,* Finite elements in fluids CIMNE Barcelona, Pineridge Press (1993), 1081-1092.

[10] F.Hecht,C.Pares, *NSP1B3: un logiciel pour resoudre les equations de Navier Stokes incompressible 3D* Rapports de Recherche INRIA, no.1449, (1991).

[11] O.C.Zienkewicz, *The finite element method in engineering science* (McGraw-Hill, New York, 1977).

[12] C.C.Mei, *The applied dynamics of ocean surface wave* (World Scientific, Singapore, 1989).

Unité de recherche INRIA Rocquencourt
Domaine de Voluceau - Rocquencourt - B.P. 105 - 78153 Le Chesnay Cedex (France)

Unité de recherche INRIA Lorraine - Technopôle de Nancy-Brabois - Campus scientifique
615, rue du Jardin Botanique - B.P. 101 - 54602 Villers lès Nancy Cedex (France)
Unité de recherche INRIA Rennes - IRISA, Campus universitaire de Beaulieu 35042 Rennes Cedex (France)
Unité de recherche INRIA Rhône-Alpes 46, avenue Félix Viallet - 38031 Grenoble Cedex 1 (France)
Unité de recherche INRIA Sophia Antipolis - 2004, route des Lucioles - B.P. 93 - 06902 Sophia Antipolis Cedex (France)

Éditeur
INRIA - Domaine de Voluceau - Rocquencourt - B.P. 105 - 78153 Le Chesnay Cedex (France)

ISSN 0249 - 6399

RR_2456